

Limitations in Small Intestinal Neuroendocrine Tumor Therapy by mTor Kinase Inhibition Reflect Growth Factor–Mediated PI3K Feedback Loop Activation via ERK1/2 and AKT

Bernhard Svejda, MD¹; Mark Kidd, PhD¹; Alexander Kazberouk, BSc¹; Ben Lawrence, MD¹; Roswitha Pfragner, PhD²; and Irvin M. Modlin, MD, PhD¹

BACKGROUND: Treatment of small intestinal neuroendocrine tumors (SINETs) with mammalian target of rapamycin (mTOR) inhibitors alone or with somatostatin analogs has been proposed as effective therapy, because both agents have been reported to exhibit antiproliferative activity. Because adenocarcinomas escape mTOR inhibition, we examined whether the escape phenomenon occurred in SINETs and whether usage of somatostatin analogs with mTOR inhibitors surmounted loss of inhibition. **METHODS:** The effects of the somatostatin analog octreotide (OCT), the mTOR inhibitor RAD001 (RAD), or the combination were evaluated in SINET cell lines (KRJ-I, H-STS) using cell viability assays, western blotting, enzyme-linked immunosorbent assay, and reverse-transcription polymerase chain reaction to assess antiproliferative signaling pathways and feedback regulation. **RESULTS:** RAD (10^{-9} M) incompletely decreased cell viability (–40% to +15%); growth escape ($P < .001$) was noted at 72 hours in both cell lines. Phosphorylated (p)mTOR/mTOR and pp70S6K/p70S6K ratios were decreased but were associated with increases in phosphorylated extracellular signal-regulated kinase (pERK)/ERK and pAKT/AKT in both cell lines, whereas phosphorylated insulin-like growth factor 1 receptor (pIGF-1R)/IGF-1R levels were elevated only in H-STS cells. Increased ($P < .05$) transcript levels for *AKT1*, *MAPK*, *mTOR*, *IGF-1R*, *IGF-1*, and *TGF β 1* were evident. OCT (10^{-6} M) itself had no significant effect on growth signaling in either cell line. An antiproliferative effect ($66 \pm 5\%$) using OCT+RAD was only noted in the KRJ-I cells ($P < .05$). **CONCLUSIONS:** SINET treatment with the mTOR inhibitor RAD had no antiproliferative effect based on activation of pAKT and pERK1/2. A combinatorial approach using OCT and RAD failed to overcome this escape phenomenon. However, differences in RAD response rates in individual NET cell lines suggested that pretreatment identification of different tumor sensitivity to mTOR inhibitors could provide the basis for individualized treatment. *Cancer* 2011;117:4141–54. © 2011 American Cancer Society.

KEYWORDS: carcinoid, octreotide, RAD001, mTOR, feedback mechanism.

Neuroendocrine tumors (NETs) are not well known, but they are as common as Hodgkin lymphoma and more common than pancreatic, gastric, esophageal, and hepatobiliary cancers.¹ Their prevalence is increasing, however, and NETs now represent approximately 2% of all malignancies.² The misconception that NETs follow a benign course has also been debunked. Only a minority of cases are amenable to curative surgery,³ and approximately half of all patients will succumb within 6 years of diagnosis.² Antiproliferative pharmacological therapy is of limited efficacy, and new agents that target proliferative cellular pathways are under investigation.

The mammalian target of rapamycin (mTor) represents an important therapeutic target in several malignancies, and mTOR pathway signaling is considered to play a crucial role in a majority of cancers.^{4,5} Recently, a combinatorial

Corresponding author: Irvin M. Modlin, MD, PhD, Yale University School of Medicine, 333 Cedar Street, P.O. Box 208062, New Haven, CT 06520-8062; Fax: (203) 737-4067; imodlin@optonline.net

¹Gastrointestinal Pathobiology Research Group, Yale University, School of Medicine, New Haven, Connecticut; ²Institute of Pathophysiology and Immunology, Center for Molecular Medicine, Medical University of Graz, Graz, Austria

The first two authors contributed equally to this article.

DOI: 10.1002/cncr.26011, **Received:** September 8, 2010; **Revised:** December 6, 2010; **Accepted:** January 31, 2011, **Published online** March 8, 2011 in Wiley Online Library (wileyonlinelibrary.com)

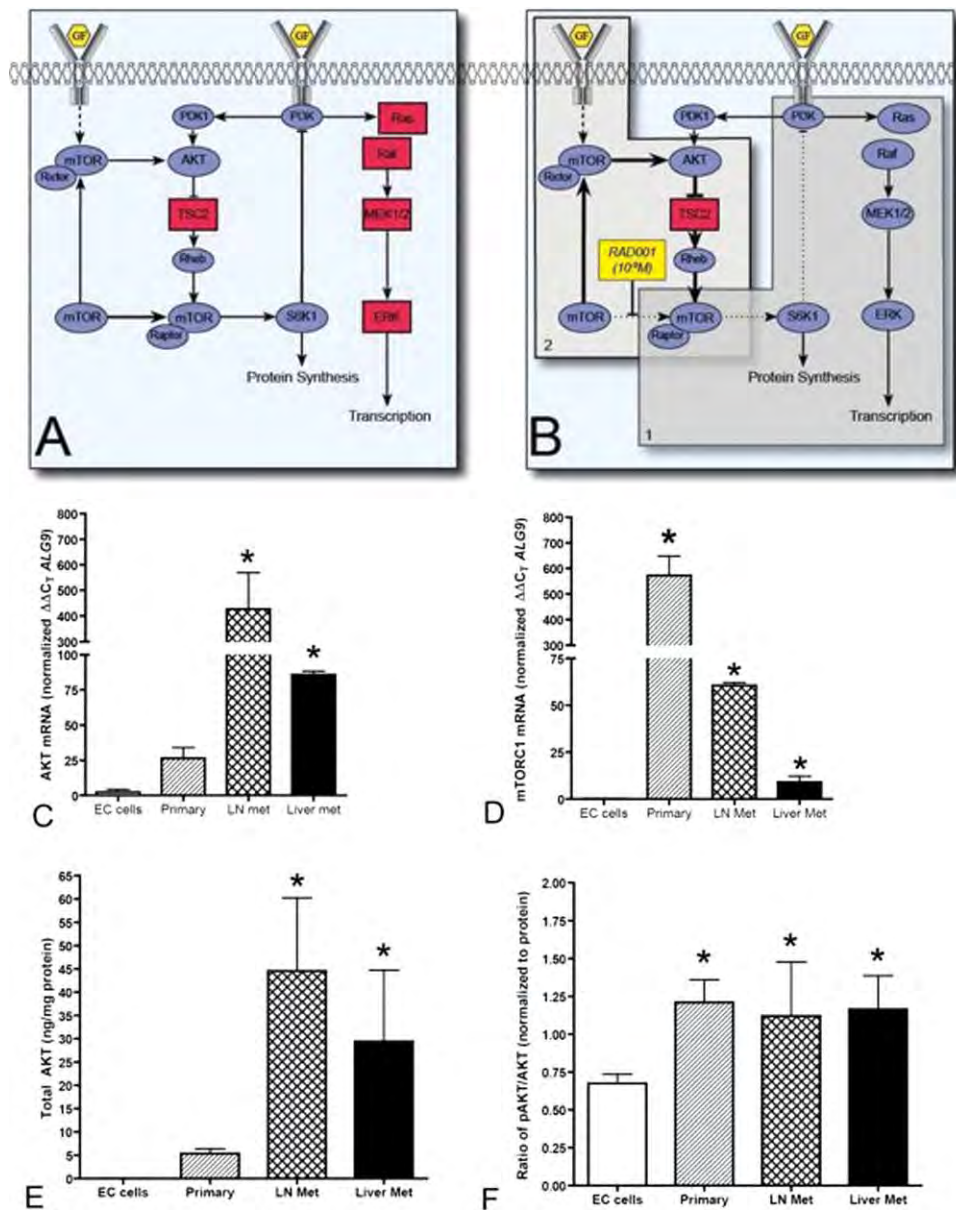


Figure 1. (A, B) Schematic of the pathways assessed in the study is shown. Briefly, mammalian target of rapamycin (mTOR)C1 leads to inhibition of phosphoinositide 3-kinase (PI3K) via the S6K1 feedback loop (A). Targeting mTOR with the mTOR inhibitor RAD001 (10^{-9} M) selectively inhibited the mTORC1 complex, whereas mTORC2 function was not affected (B, panel 2). Up-regulation of the insulin-like growth factor 1 receptor (IGF-1R)-IGF-1-PI3K pathway increased activity of Ras-Raf-extracellular signal-regulated kinase (ERK) (B, panel 1). (C-G) Transcript levels (AKT, mTORC1) and protein levels (AKT, phosphorylated AKT/total AKT) are shown for enterochromaffin (EC) cells ($n = 8$) and primary tumor-derived ($n = 3$), lymph node metastatic ($n = 3$), and liver metastatic cell lines ($n = 3$). * $P < .01$ vs normal EC cells.

approach using somatostatin analogs and mTOR inhibitors in pancreatic NET treatment has generated substantial clinical interest.^{6,7}

mTOR signaling is based on 2 distinct complexes (Fig. 1A). As a component of the mTORC1 complex, consisting of the mTOR protein and Raptor, cellular pro-

tein translation is increased after stimulation with growth factors via p70S6K and 4EBP1.⁸⁻¹¹ mTORC1 function is regulated within the phosphoinositide 3-kinase (PI3K)/AKT pathway by inhibition of the guanosine triphosphatase activity of tuberous sclerosis complex 2 (TSC2), which controls activity of the mTOR activator Rheb.¹²⁻¹⁴

In contrast, mTOR associated with Rictor in the mTORC2 complex responds to growth factor receptor binding, which leads to full activation of AKT kinase by phosphorylation at the Ser473 side.^{11,15,16} mTOR inhibitors (eg, rapamycin, everolimus [RAD001]) selectively inhibit mTORC1 at concentrations at the low nanomolar range, mTORC2 inhibition generally requires doses in the micromolar concentrations, levels that are $\approx 10^3$ -fold higher than those achieved in clinical treatment.^{4,17} In general, clinical trials performed with rapamycin derivatives have turned out to be less successful than predicted by *in vitro* data. In recent studies, it has been demonstrated that a negative mTORC1/AKT feedback loop increases AKT activity via an increase in receptor tyrosine kinase (RTK)/insulin receptor substrate 1 (IRS-1).¹⁸⁻²² In addition, a negative feedback loop occurs via the p70S6K-Ras pathway, which causes cross-activation of the Ras-Raf-ERK pathway after mTOR inhibitor treatment.^{23,24}

High expression rates of phosphorylated (p)mTOR have been demonstrated in poorly differentiated NETs, suggesting a potential role of mTOR inhibitors in NET treatment.²⁵ Additionally, a comparative *in vitro* study in NET cell lines of pancreatic, midgut, and bronchial origin suggested feedback activation in the liver metastasis-derived small intestinal NET (SINET) cell line GOT1.²⁶ However, the phenomenon of mTOR inhibitor escape has neither been examined in a primary tumor-derived SINET cell line nor in the presence of a somatostatin analog. We hypothesized that in SINETs, the combination of mTOR inhibition and a somatostatin analog would overcome any potential cell proliferation escape phenomena and exceed the antiproliferative effect of either drug alone. Accordingly, we investigated the effects of RAD001, the somatostatin analog octreotide, or the combination of both drugs on cell proliferation, activation of the PI3K-AKT-mTOR pathway, activation of the Ras-Raf-ERK pathway, and the production of growth factors and their receptors in primary and metastatic SINET cell lines.

MATERIALS AND METHODS

Cell Lines and Enterochromaffin Cell Isolation

Normal small intestinal enterochromaffin (EC) cells were isolated as described; $\approx 1 \times 10^6$ cells were obtained per sample.²⁷ The SINET cell lines KRJ-I, P-ST5 (both primary tumors), H-ST5 (liver metastasis), and L-ST5 (lymph node metastasis) were cultured as described.²⁸⁻³² All experiments were performed without antibiotics.

Chemicals

Octreotide LAR (OCT) and RAD001 (RAD) were a kind gift from Novartis AG (Basel, Switzerland).

Proliferation Studies

2×10^5 cells/mL, seeded in 96-well plates at 100 μ L were stimulated with RAD (10^{-6} to 10^{-12} M, $n = 6$ wells/concentration) and OCT (10^{-6} to 10^{-12} M, $n = 6$ wells/concentration).^{29,30,33} After 72 hours of incubation, cell viability was analyzed using MTT as described.^{33,34} Results were normalized to the unstimulated control, and the effective half-maximal concentrations were calculated.

To evaluate the combination of OCT and RAD, KRJ-I and H-ST5 cells were seeded as described above and stimulated with OCT (10^{-6} M), RAD (10^{-9} M), or the combination. Cell viability was measured after 24, 48, and 72 hours using WST-1 cell proliferation reagent according to the manufacturer's instructions.³⁵ Optical density was quantified photospectrometrically at 450 nm using a microplate reader (Bio-Rad 3500). Results ($n = 6$) were normalized to control, and effects between different drugs were analyzed by way of unpaired *t* tests.

pAKT/AKT Signaling Pathway Analysis

After 24 hours of incubation, AKT signal activity was evaluated in normal small intestinal EC cells and in the KRJ-I, P-ST5, H-ST5, and L-ST5 cell lines using Super-Array CASE enzyme-linked immunosorbent assay (ELISA) kits (SA Biosciences, Frederick, Md) according to the manufacturer's instructions.^{29,30}

Protein Extraction

KRJ-I and H-ST5 cells (4×10^5 cells/mL) were seeded in 6-well plates (Falcon; BD, Franklin Lakes, NJ) and treated with OCT (10^{-6} M), RAD (10^{-9} M) or the combination for 24 hours. After cells were harvested, whole-cell lysates were prepared by adding 200 μ L of ice-cold cell lysis buffer ($10 \times$ RIPA lysis buffer [Millipore, Billerica, Mass], complete protease inhibitor [Roche, Indianapolis, Ind], phosphatase inhibitor sets 1 and 2 [Calbiochem, Gibbstown, NJ], 100 mM phenylmethanesulfonyl fluoride [Roche], 200 mM Na_3VO_4 [Acros Organics], 12.5 mg/mL sodium dodecyl sulfate [SDS] [American Bioanalytical, Natick, Mass]). Tubes were centrifuged at 12,000 g for 20 minutes, and supernatant protein was quantified (BCA protein assay kit; Thermo Fisher Scientific, Rockford, Ill).

Western Blot Analysis

Total protein lysates (20 μ g) were denatured in SDS sample buffer, separated by way of SDS–polyacrylamide gel electrophoresis (4, 10%), and transferred to a polyvinylidene fluoride membrane (Bio-Rad, Hercules, Calif, pore size 0.45 mm). After blocking (5% bovine serum albumin for 60 minutes at room temperature), membranes were incubated with primary antibodies (Cell Signaling Technology, Danvers, Mass) in 5% bovine serum albumin/phosphate-buffered saline/Tween 20 overnight at 4°C, then with horseradish peroxidase–conjugated secondary antibodies (Cell Signaling Technology) for 60 minutes at room temperature, and immunodetection was performed using the Western Lightning Plus-ECL (PerkinElmer, Mass). Blots were exposed on X-OMAT-AR films.³⁶ Cross-detection between pAKT (Ser473) and AKT, phosphorylated tuberlin (Thr1462) and tuberlin, pp70S6K (Thr389) and p70S6K, pmTOR (Ser2448) and mTOR, pERK1/2 (Thr185, Tyr187) and ERK1/2, TGF β 2-receptor (TGF β 2-R), and phosphorylated IGF-1 β receptor (pIGF-1R) (Tyr1316) and IGF-1R was avoided by stripping the membranes. The optical density of the appropriately sized bands was measured using ImageJ software (National Institutes of Health, Bethesda, Md). The ratio between phosphorylated protein and total protein was calculated, and total protein expression was reported relative to that of β -actin (Sigma-Aldrich, Mo).

RNA Isolation and Reverse Transcription

RNA was extracted from each cell line (1×10^6 , $n = 6$) using TRIzol (Invitrogen, Carlsbad, Calif) and cleaned (Qiagen, RNeasy kit, Qiagen, Valencia, Calif). After conversion to complementary DNA (High Capacity cDNA Archive Kit; Applied Biosystems, Carlsbad, Calif),^{28,37} reverse-transcription polymerase chain reaction (RT-PCR) analyses were performed using Assays-on-Demand and the ABI 7900 Sequence Detection System.^{28,37} Primer sets were obtained from Applied Biosystems, and PCR mix on gels were performed to confirm presence of single bands for each primer set. PCR data were normalized using the $\Delta\Delta C_T$ method; *ALG9* was used as a housekeeping gene.³⁸

5-Hydroxytryptamine, Insulin-Like Growth Factor 1, and Transforming Growth Factor β 1 Secretion

Levels of 5-hydroxytryptamine (5-HT), insulin-like growth factor 1 (IGF-1), and transforming growth factor β 1 (TGF β 1) were analyzed using commercially available

ELISA assays (5-HT, BA 10-0900, Rocky Mountain Diagnostics; TGF β 1, DB100B, R&D Systems; IGF-1, R&D Systems).^{27,28} Briefly, cells were seeded into 6-well plates ($n = 6$) and stimulated with OCT (10^{-6} M), RAD (10^{-9} M), or the combination, and agent levels were measured after 24 hours.

Statistical Analysis

All statistical analyses were performed using Microsoft Excel and Prism 4 (GraphPad Software, San Diego, Calif). Nonlinear regression analyses were used to identify half-maximal inhibitory (IC_{50}) concentrations. Cell viability tests were analyzed using a Student *t* test; all other data were assessed using 2-tailed, unpaired *t* tests.

RESULTS

mTOR and AKT Pathway Activation in Untreated Cell Lines

Transcription of AKT and *mTORC1*

Transcript levels of *AKT* and *mTORC1* were analyzed in normal EC cells and in primary tumor–derived (KRJ-I, P-ST5), lymph node metastatic (L-ST5), and liver metastatic cell lines (H-ST5) using RT-PCR. No significant difference in *AKT* messenger RNA levels was noted between normal EC cells and both primary tumor–derived cell lines, whereas increased transcript levels were determined in the lymph node and liver metastasis cell lines ($P < .05$). In contrast, *mTORC1* transcripts were present at very low levels in normal EC cells but were significantly increased in each of the cell lines ($P < .05$) (Fig. 1C, D).

Protein levels of total AKT as well as pAKT/AKT

We next quantified protein levels of AKT and determined the ratio of pAKT to total AKT. Levels of SINET cell lines were compared with normal EC cells. AKT protein was identified in all tumor cell lines and was notably increased in metastatic cell lines ($P < .05$). The ratio of pAKT/AKT was significantly elevated in all tumor cell lines ($P < .05$) compared with normal EC cells (Fig. 1E, F).

Effects on SINET Cell Viability After RAD and OCT Administration

Dose-dependent effects of RAD and OCT on cell viability

Having determined that *mTORC1* was expressed in the cell lines and that the AKT signaling pathway was activated, we evaluated the effects of RAD and OCT on

72-hour cell viability. Targeting mTOR with RAD significantly inhibited viability (20%-50%; $IC_{50} < 0.3$ nM; $P < .05$). This effect was most evident in the metastatic cell lines (L-STS, $IC_{50} = 2.3 \times 10^{-11}$ M; H-STS, $IC_{50} = 2.1 \times 10^{-11}$ M; $P < .05$) with a maximum inhibitory effect of $52 \pm 2\%$ (Fig. 2A-D). After OCT administration, an antiproliferative effect was noted in the 2 primary tumor-derived cell lines (KRJ-I, P-STS) and the lymph node metastasis-derived cell line (L-STS) (KRJ-I, $IC_{50} = 1.7 \times 10^{-11}$ M; P-STS, $IC_{50} = 7.9 \times 10^{-9}$ M; L-STS, $IC_{50} = 1.1 \times 10^{-8}$ M), with a maximum effect of $73 \pm 6\%$ and $82 \pm 4\%$ (Fig. 2A-D); no effect was evident in the liver metastatic cell line.

Effects of RAD in combination with OCT on cell viability

To evaluate the efficiency of a dual inhibitory approach targeting somatostatin receptors and mTOR, effects of OCT and RAD were determined in KRJ-I, P-STS, L-STS, and H-STS cells. OCT (10^{-6} M) had a modest inhibitory effect ($\approx 5\%$ - 10% inhibition, $P < .05$) on cell proliferation in KRJ-I and L-STS cells. In primary tumor-derived cell lines, the combination of RAD (10^{-9} M) and OCT (10^{-6} M) was significantly more effective ($P < .05$) than treatment with each agent alone. The combinatorial treatment exhibited no significant effect in the metastatic-derived cells lines L-STS and H-STS (Fig. 2E-H).

Time response of RAD and OCT treatment on cell viability

To examine the phenomenon of growth escape, the antiproliferative effects of each agent were determined in KRJ-I and H-STS cells after 24, 48, and 72 hours (Fig. 2I, J). After administration of OCT, a significant decrease in cell viability was noted in the primary-derived cell line (KRJ-I) ($85 \pm 5\%$, $P < .001$), whereas no antiproliferative effect was obvious in the liver metastasis-derived cell line ($109 \pm 5\%$, $P < .001$). A significant decrease was noted after RAD treatment in both tumor cell lines at 24 and 48 hours (KRJ-I, $78 \pm 4\%$, $47 \pm 4\%$; H-STS, $60 \pm 5\%$, $55 \pm 3\%$; $P < .001$), but after 72 hours an increase of cell viability was observed (KRJ-I, $95 \pm 5\%$; H-STS, $82 \pm 10\%$; $P < .001$). Combination of both drugs enhanced antiproliferative effects in both tumor cell lines at 24 and 48 hours of treatment (KRJ-I, $63 \pm 5\%$, $38 \pm 0.6\%$; H-STS, $49 \pm 0.3\%$, $48 \pm 0.3\%$; $P < .001$). However, an increase of cell viability was noted after combinatorial treatment for 72 hours compared with 24 and 48

hours (KRJ-I, $78 \pm 9\%$; H-STS, $80 \pm 12\%$; $P < .001$). An additional antiproliferative effect was only evident in KRJ-I cells after combined treatment ($P < .001$).

mTOR and AKT Pathway Activation After Treatment With RAD and OCT

Protein levels of mTOR, TSC2, p70S6K, ERK, AKT, and IGF-1 receptor at 24 hours

Because one of the drawbacks of mTOR inhibition is cross-reactivation of the AKT pathway as well as the ERK1/2 pathway, we evaluated the effects of RAD, OCT, and the combination on AKT, TSC2, p70S6K, ERK1/2, and IGF-1R phosphorylation in KRJ-I and H-STS cells.

Effects on AKT activity.

A significant decrease in pAKT (Ser473) was noted in KRJ-I cells after treatment with OCT and OCT+RAD. This finding did not translate into differences in the pAKT/AKT ratio (a measure of pathway activation), indicating incomplete inhibition of pAKT/AKT activity after RAD administration in this cell line (Fig. 3). No effects were observed after OCT treatment compared with untreated controls. In H-STS, a significant increase in pAKT (Ser473) protein levels was determined after administration of OCT+RAD and was accompanied by a decrease in total AKT. The ratio of pAKT/AKT was significantly higher in RAD and OCT+RAD treated with H-STS cells ($141 \pm 14\%$, $183 \pm 34\%$; $P < .05$) (Fig. 4). No effects were noted after OCT treatment.

Effects on TSC2 activity.

RAD and OCT+RAD significantly increased pTSC2 (Thr1462) levels in KRJ-I cells and were accompanied by a decrease in total TSC2. The pTSC2/TSC2 ratio was significantly elevated after treatment with RAD and OCT+RAD ($539 \pm 92\%$, $868 \pm 121\%$; $P < .05$) (Fig. 3). In H-STS cells, levels of pTSC2 (Thr1462) were increased after RAD and OCT+RAD administration, with a significant decrease in total protein. The ratio of pTSC2/TSC2 was increased by RAD and OCT+RAD ($429 \pm 64\%$, $532 \pm 68\%$, $P < .05$) (Fig. 4). No significant differences for OCT were noted in either cell line.

Effects on mTOR activity.

In KRJ-I cells, a significant decrease in pmTOR (Ser2448) was noted after RAD and OCT+RAD treatment and was associated with a decrease in total protein levels. The ratio of pmTOR/mTOR was significantly lower after RAD and OCT+RAD ($85 \pm 3\%$, $82 \pm 6\%$, $P < .05$)

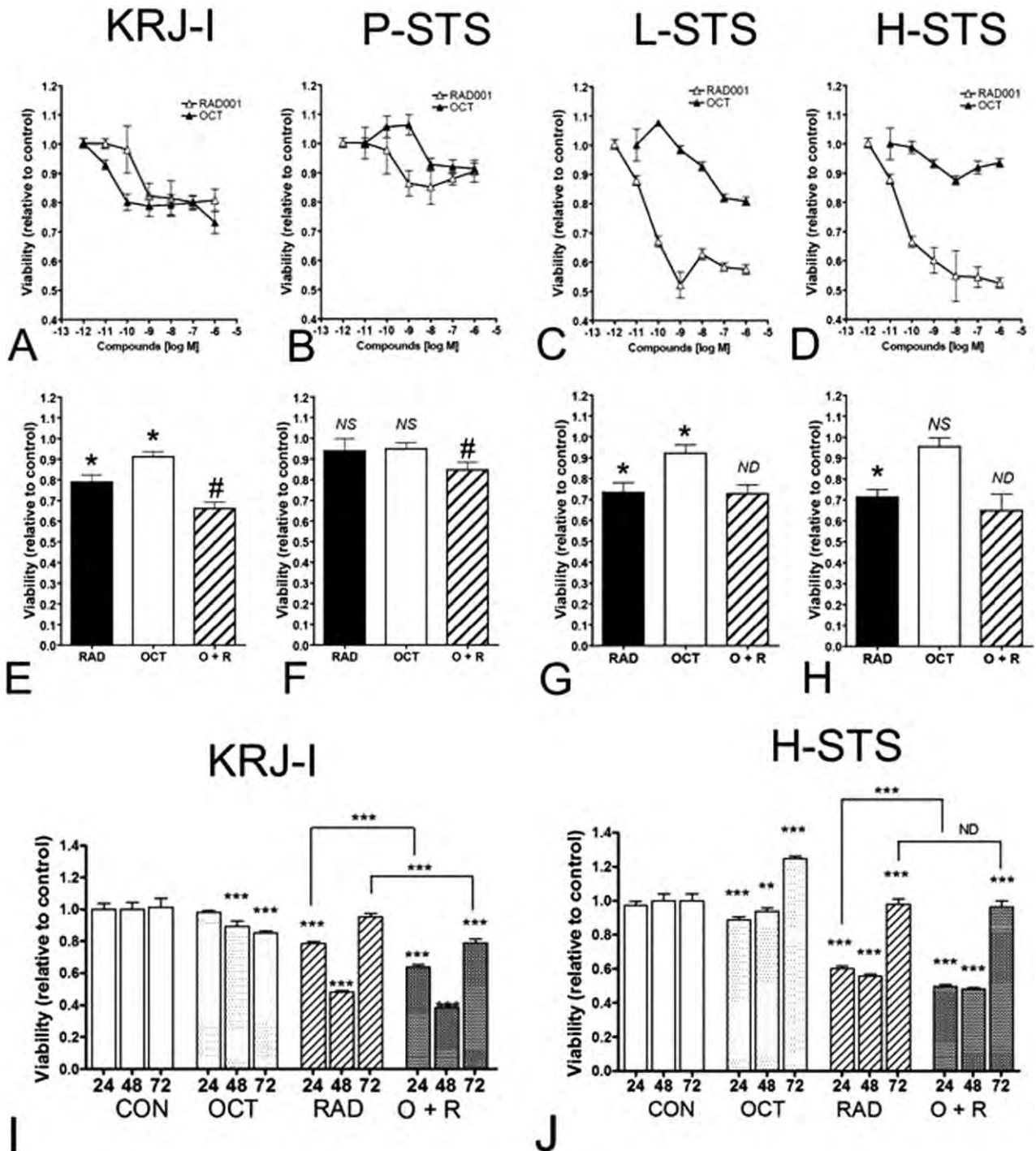


Figure 2. (A-D) Dose-dependent viability response in primary (KRJ-I, P-STs) and metastatic (L-STs, H-STs) cell lines after 72 hours with RAD001 (RAD) and octreotide (OCT) treatment is shown. (E-H) Effects of RAD (10^{-9} M), OCT (10^{-6} M), and the combination (O+R) after 72 hours of treatment is shown. (I, J) Time-dependent viability response in primary (KRJ-I) and liver metastatic (H-STs) cell lines after 24, 48, and 72 hours of OCT (10^{-6} M), RAD (10^{-9} M), and the combination (O+R) is shown. NS indicates not significant; ND, not different. * $P < .05$, ** $P < .01$, *** $P < .001$, # $P < .05$ vs RAD. Data are expressed as the mean \pm SEM (n = 12).

KRJ-I

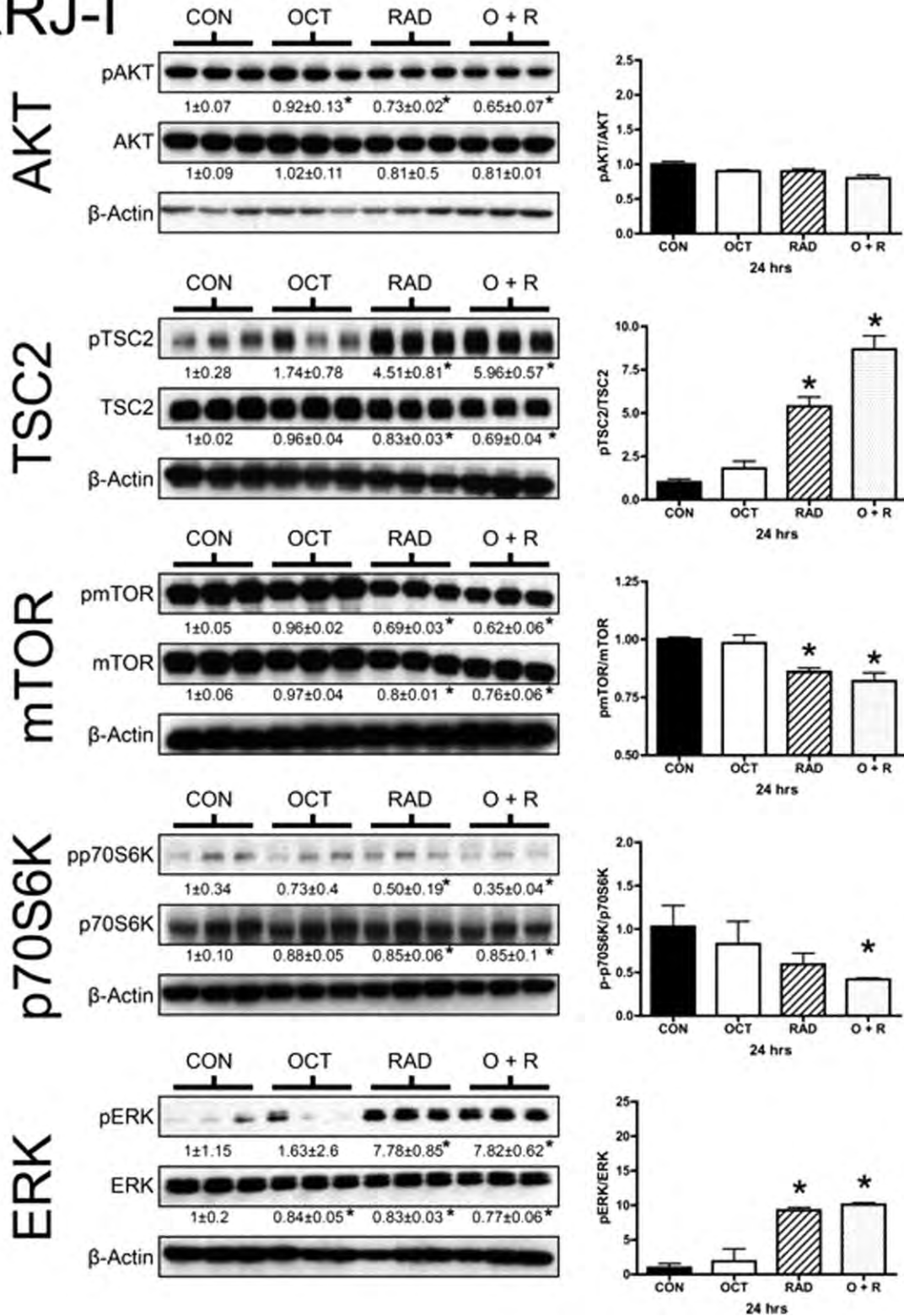


Figure 3. Western blot analysis of AKT, tuberous sclerosis complex 2 (TSC2), mammalian target of rapamycin (mTOR), p70S6K, and extracellular signal-regulated kinase (ERK)1/2 in KRJ-I cells after 24 hours of octreotide (OCT, 10^{-6} M), RAD001 (RAD, 10^{-9} M), and octreotide+RAD001 (O+R) is shown. Levels of phosphorylated as well as total protein are shown normalized to β -actin (left panels). The ratio of phosphorylated versus total protein is depicted in the right panel. * $P < .05$ vs control. Data are expressed as the mean \pm SEM ($n = 3$).

H-STS

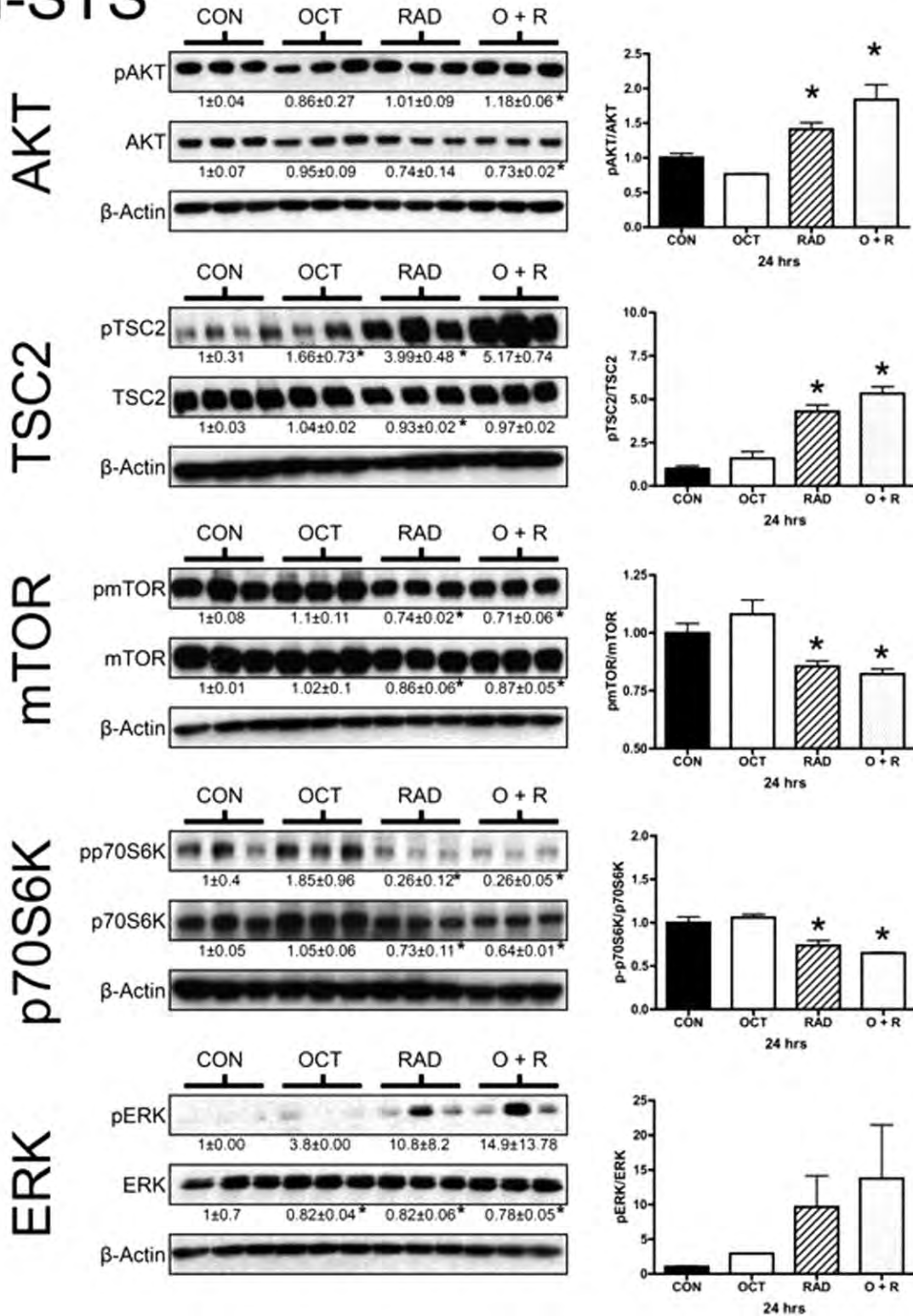


Figure 4. Western blot analysis of AKT, tuberous sclerosis complex 2 (TSC2), mammalian target of rapamycin (mTOR), p70S6K, and extracellular signal-regulated kinase (ERK) 1/2 in H-STS cells after 24 hours of octreotide (OCT, 10^{-6} M), RAD001 (RAD, 10^{-9} M), and octreotide+RAD001 (O+R) is shown. Phosphorylated protein as well as total protein is depicted normalized to levels of β -actin (left panel). The ratio of phosphorylated versus total protein is demonstrated in the right panel. * $P < .05$ vs control. Data are expressed as the mean \pm SEM ($n = 3$).

compared with untreated controls (Fig. 3). In H-STS cells, a significant decrease in pmTOR (Ser2448) was noted with RAD and OCT+RAD associated with a decrease in total protein. The ratio of pmTOR/mTOR was significantly decreased by RAD and OCT+RAD ($85 \pm 4\%$, $82 \pm 3\%$, $P < .05$) (Fig. 4). No significant effect was evident for OCT in either cell line.

Effects on p70S6K activity.

A significant decrease in pp70S6K (Thr389) was noted in KRJ-I cells after treatment with RAD and was associated with a decrease in total protein. The ratio of pp70S6K and p70S6K was significantly decreased by OCT+RAD ($42 \pm 2\%$, $P < .05$) (Fig. 3). In H-STS, pp70S6K (Thr389) was decreased after RAD and OCT+RAD administration along with a decrease in total protein. No effect was observed for OCT treatment. A significant reduction of pp70S6K/p70S6K ratio was noted for RAD and OCT+RAD ($73 \pm 10\%$, $64 \pm 1\%$; $P < .05$) (Fig. 4). No effect was evident after OCT treatment in either cell line.

Effects on ERK1/2 activity.

A significant increase of pERK1/2 (Thr185, Tyr187) was noted in KRJ-I cells after RAD and OCT+RAD treatment, accompanied by a decrease in total protein. The ratio of pERK1/2 and ERK1/2 was significantly increased by RAD and OCT+RAD ($928 \pm 71\%$, $1012 \pm 101\%$; $P < .05$) (Fig. 3). In H-STS cells, an increase of pERK1/2 (Thr185, Tyr187) was observed after RAD and OCT+RAD administration, accompanied by a decrease in total protein. The ratio of pERK1/2 and ERK1/2 was increased after RAD and OCT+RAD treatment (Fig. 4). No effects were noted after OCT administration in either cell line.

Effects on IGF-1 receptor activity.

Whereas no significant effects of either agent were noticed in KRJ-I cells, pIGF-1R levels (Tyr1316) were significantly elevated in H-STS cells after RAD treatment, accompanied by an increase in total IGF-1R protein (Fig. 5). After OCT administration, a decreased protein amount of IGF-1R was evident. The ratio of pIGF-1R/IGF-1R was significantly increased after RAD treatment ($128 \pm 15\%$, $P < .05$) (Fig. 5).

Transcript levels of Ki67, mTOR, AKT1, and MAPK1

Transcript analyses of *Ki67*, *mTOR*, *AKT1*, and *MAPK1* (*ERK1*) in KRJ-I and H-STS cells was examined

24 hours after treatment with OCT (10^{-6} M), RAD (10^{-9} M), and OCT+RAD using RT-PCR. In KRJ-I and H-STS cells, transcript levels for *Ki67* were significantly decreased after treatment with RAD ($53 \pm 1.2\%$, $P < .001$; $86 \pm 11\%$, $P < .05$) and the combination of RAD+OCT ($65 \pm 8.5\%$, $P < .001$; $87 \pm 12\%$, $P < .05$), whereas a significant increase was evident after OCT administration alone ($123 \pm 10\%$, $P < .01$; $124 \pm 8.2\%$, $P < .001$) (Fig. 6A). After RAD treatment, a significant increase in transcripts for *mTOR* (KRJ-I, $120 \pm 4.9\%$, $P < .05$; H-STS, $126 \pm 4.1\%$, $P < .001$), *AKT1* (KRJ-I, $119 \pm 9.3\%$; H-STS, $143 \pm 27\%$; $P < .05$), and *MAPK1* (KRJ-I, $130 \pm 10\%$, $P < .001$; H-STS, $119 \pm 8\%$, $P < .01$) levels were noted. In KRJ-I and H-STS cells, similar observations were evident after the combinatorial treatment (*mTOR*, $128 \pm 13\%$, $135 \pm 16\%$, $P < .05$; *AKT1*, $124 \pm 14\%$, $137 \pm 19\%$, $P < .01$; *MAPK1*, $132 \pm 15\%$, $127 \pm 4.2\%$, $P < .001$) (Fig. 6B-D, F-H). No significant differences were noted after OCT treatment except for an increase in *AKT1* levels in H-STS cells ($148 \pm 31\%$, $P < .01$) (Fig. 6G).

Growth Factor Secretion and Transcription in SINET Cells After RAD and OCT Treatment

Effects of OCT (10^{-6} M), RAD (10^{-9} M) and the combination on 5-HT, IGF-1, and TGF β 1 secretion were evaluated in KRJ-I and H-STS cells using ELISA. A significant decrease in 5-HT secretion was evident in KRJ-I cells treated with all compounds (OCT, $57 \pm 26\%$; RAD, $63 \pm 27\%$; OCT+RAD, $68 \pm 23\%$; $P < .05$), whereas only a significant effect of OCT was noted in H-STS (OCT, $52 \pm 26\%$; $P < .05$). IGF-1 secretion was significantly elevated in KRJ-I and H-STS cells by OCT ($128 \pm 21\%$, $113 \pm 8\%$; $P < .05$), RAD ($141 \pm 29\%$, $118 \pm 12\%$; $P < .05$), and OCT+RAD ($125 \pm 22\%$, $118 \pm 6\%$; $P < .05$) compared with untreated controls. No significant effects in TGF β 1 secretion were noted (Fig. 7A-F).

Growth factor receptor transcripts for *IGF-1R* and *TGF β 2-R* as well as transcripts for *IGF-1* and *TGF β 1* were evaluated after 24 hours of treatment with OCT (10^{-6} M), RAD (10^{-9} M), and OCT+RAD using RT-PCR (Fig. 5A-H). A significant increase in *IGF-1R* transcript levels was noted in both cell lines after RAD and OCT+RAD treatment (KRJ-I, $178 \pm 49\%$, $P < .01$, $173 \pm 22\%$, $P < .001$; H-STS, $185 \pm 11\%$, $187 \pm 18\%$, $P < .001$), accompanied by elevated levels for *IGF-1* transcripts (KRJ-I, $185 \pm 48\%$, $189 \pm 57\%$, $P < .05$; H-STS, $235 \pm 78\%$, $P < .05$, $199 \pm 45\%$, $P < .001$). *TGF β 2-R*

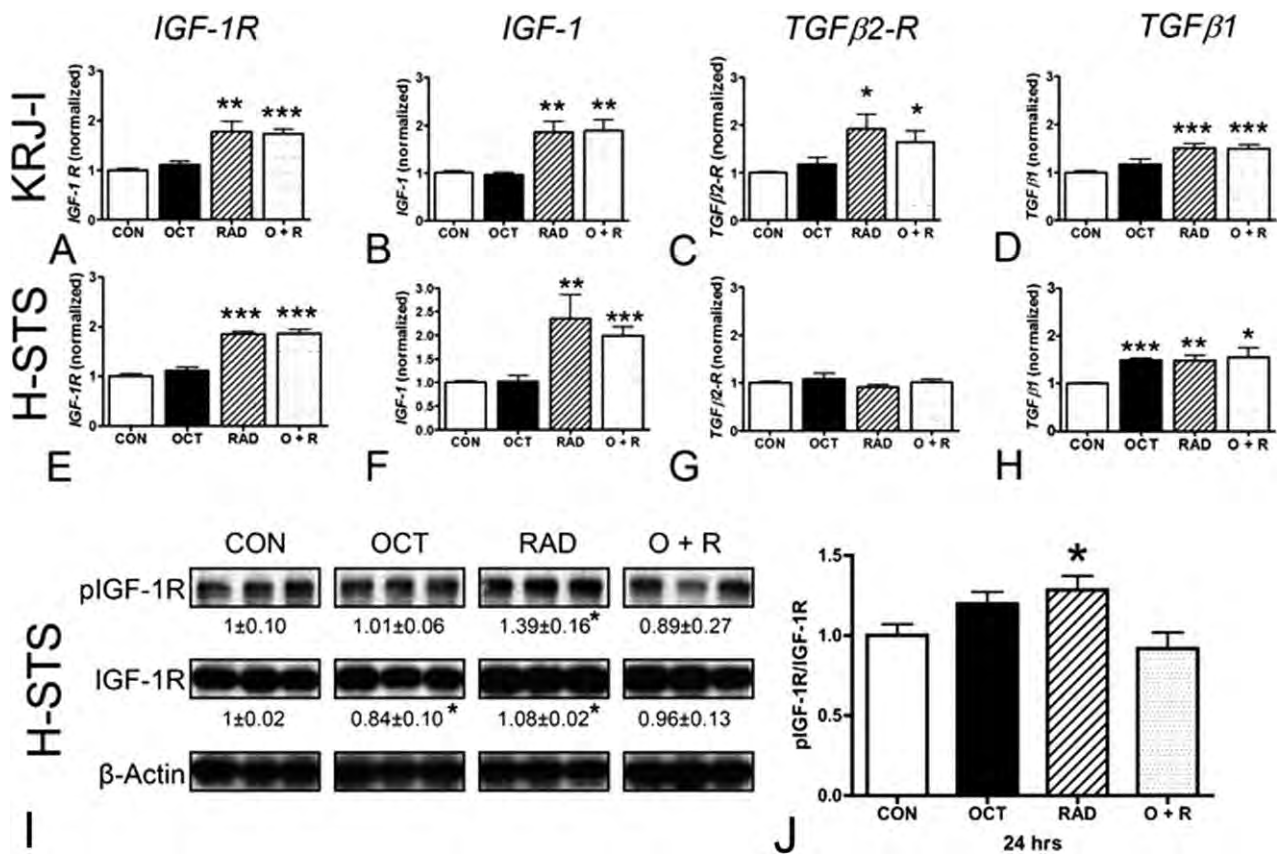


Figure 5. (A-H) Transcript levels of insulin-like growth factor 1 receptor (IGF-1R), IGF-1, transforming growth factor β2 receptor (TGFβ2-R), and TGFβ1 after 24 hours of treatment with octreotide (OCT, 10⁻⁶ M), RAD001 (RAD, 10⁻⁹ M), and octreotide+RAD001 (O+R) for KRJ-I and H-STC cells are shown. (I, J) Western blot analysis of IGF-1R in H-STC cells after 24 hours of treatment with OCT (10⁻⁶ M), RAD (10⁻⁹ M), and O+R. Levels of phosphorylated, total protein, and the ratio are depicted. **P* < .05, ***P* < .01, ****P* < .001. Data are expressed as the mean ± SEM (n = 6).

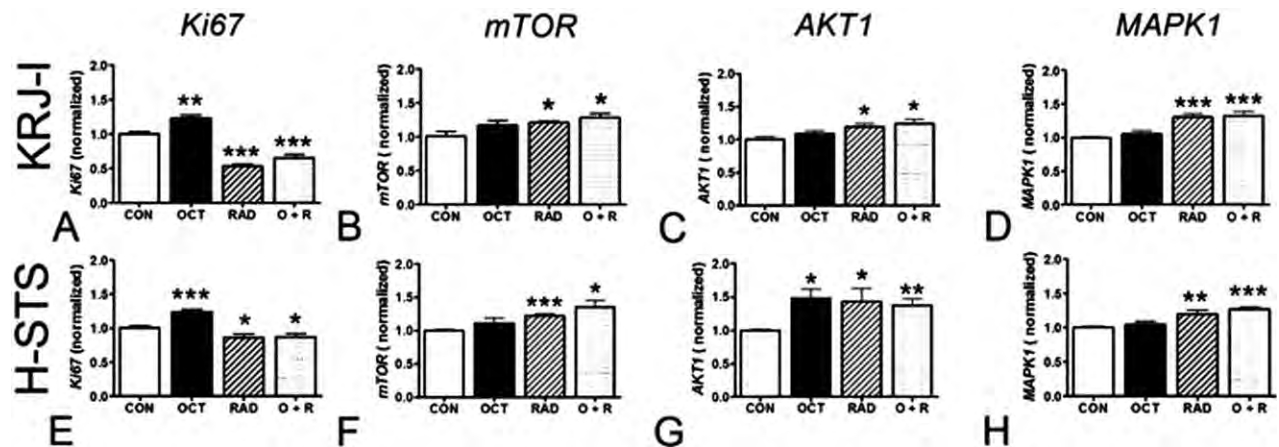


Figure 6. Effects of octreotide (OCT), RAD001 (RAD), and octreotide+RAD001 (O+R) on Ki67, MAPK1, mammalian target of rapamycin (mTOR), and AKT1 transcripts in KRJ-I (primary tumor) and H-STC (liver metastasis) are shown. **P* < .05, ***P* < .01, ****P* < .05. Data are expressed as the mean ± SEM (n = 3).

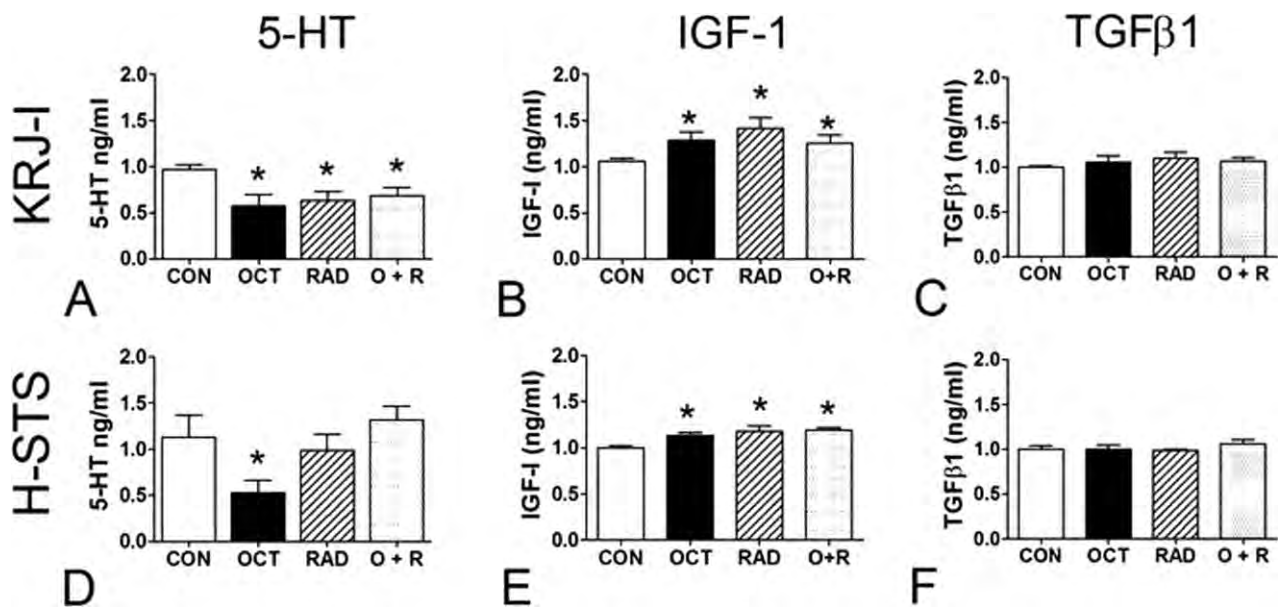


Figure 7. Effects of octreotide (OCT, 10^{-6} M), RAD001 (RAD, 10^{-9} M), and octreotide+RAD001 (O+R) on 5-hydroxytryptamine (5-HT) (A, D), insulin-like growth factor 1 (IGF-1) (B, E), and transforming growth factor β 1 (TGF β 1) (C, F) secretion in KRJ-I and H-ST5 cells are shown. * $P < .05$. Data are expressed as the mean \pm SEM ($n = 6$).

levels were significantly increased in KRJ-I cells after RAD and OCT+RAD treatment ($191 \pm 71\%$, $164 \pm 48\%$; $P < .05$); no differences were evident in H-ST5 cells. Both RAD and OCT+RAD significantly elevated transcript levels for *TGF β 1* in KRJ-I and H-ST5 cells (KRJ-I, $150 \pm 23\%$, $149 \pm 20\%$, $P < .001$; H-ST5, $148 \pm 27\%$, $155 \pm 48\%$, $P < .05$). No differences were noted after OCT treatment except for an increase in *TGF β 1* levels in H-ST5 cells ($149 \pm 8.6\%$; $P < .001$).

DISCUSSION

High expression rates of pmTOR have been demonstrated in poorly differentiated NETs, suggesting a potential role of mTOR inhibitors in NET treatment.²⁵ In the current study, the PI3K-AKT-mTOR pathway was significantly elevated in SINETs in both primary tumors as well as in lymph node and liver metastasis, suggesting a crucial role in tumor proliferation and progression. The role of this pathway is likely neoplasia-related, because normal EC cells exhibit very low expression of transcripts for *AKT* and *mTORC1*, as well as for AKT signaling. SINETs are therefore potentially treatable by targeting the mTOR with selective inhibitors. A combinatorial approach with the somatostatin analog OCT, which has been demonstrated to lengthen time to tumor progression,³⁹ could potentially result in an increased antiproliferative effect in

SINETs. In the current study, we present the effects of RAD and OCT in primary tumor-derived as well as lymph node-derived and liver metastasis-derived SINET cell lines.

OCT only decreased cell viability in primary tumors and lymph node metastasis, whereas the antiproliferative effect of RAD was noted in every cell line regardless of the site; this effect was more evident in metastatic cell lines compared with primary tumors. This finding suggests that a combinatorial approach of OCT and RAD might result in an augmented antiproliferative effect in disseminated NET disease. However, an increased antiproliferative response using OCT and RAD in combination was only evident in the primary tumor cell line, whereas no effect was noted in the metastases.

We next evaluated mechanistic basis of the cellular responses by assessing cell viability at 24, 48, and 72 hours using RAD, OCT, and OCT+RAD at concentrations typically reached in clinical treatment (RAD, 10^{-9} M; OCT, 10^{-6} M). Whereas a significant decrease in cell viability was noted in the primary-derived cell line KRJ-I treated with OCT, no antiproliferative effect was noted in the liver metastasis-derived cell line H-ST5, indicating that treatment with OCT demonstrates a beneficial antiproliferative effect only in the primary-derived tumor. RAD exhibited a significant antiproliferative response after 24 and 48 hours in primary and liver metastasis-

derived cell lines. However, an increase in cell viability to levels similar to those at pretreatment was evident after 72 hours of RAD administration, suggesting that tumor cells escape biotherapeutic treatment. The combinatorial approach did not reverse this growth-regulatory escape phenomenon. These findings indicate that targeting mTOR in SINETs subsequently results in growth escape, either through feedback mechanisms within the PI3K–AKT–mTOR pathway or through cross-activation of other crucial cell survival pathways.

A negative feedback loop by inhibition of mTORC1 has been demonstrated to increase levels and activity of the growth factor receptor adaptor protein, IRS-1, which was mediated via the mTORC1 target p70S6K, resulting in Ras–Raf–ERK pathway activation.^{19,24} In our study, targeting SINETs with RAD significantly decreased phosphorylated mTOR and lowered the ratio of phosphorylated versus total mTOR protein in the primary tumor cell line KRJ-I, as well as in the liver metastasis cell line H-STS, an effect that was accompanied by a decrease in p70S6K. Due to the deregulated negative feedback loop of p70S6K, a significant increase of pERK1/2 activity was evident in both cell lines after RAD administration (Figure 1B, panel 1). Our findings demonstrate tumor cell escape in RAD-treated SINETs by cross-activation of the ERK1/2 pathway resulting in resistance to mTOR inhibitor treatment.

Whereas mTORC1 is preferentially inhibited at rapamycin concentrations in the nM range, mTORC2 can only be successfully blocked by dose rates at the micromolar level.¹⁷ mTORC2 plays a crucial role in an mTORC1/AKT feedback loop by selective activation of AKT at Ser473, and treatment with mTOR inhibitors has been demonstrated to cause a strong inhibition, a partial inhibition, or an increase in AKT phosphorylation.^{16,40} In the SINET cell lines, AKT phosphorylation as well as pAKT/AKT levels were significantly increased in H-STS cells, whereas in treated KRJ-I cells, pAKT levels exhibited no significant differences compared with controls. This finding was accompanied by a significant increase in pTSC2 levels in both tumor cell lines, which has been demonstrated to activate mTORC1 via Rheb.^{13,14,16} Increased transcript levels of *mTOR*, *AKT1*, and *MAPK1* confirmed these western blot results. Consequently, targeting mTORC1 with RAD in the nM range increased mTORC2 activity, which resulted in either activation (H-STS) or incomplete inhibition (KRJ-I) of AKT phosphorylation, with consequent resistance to mTOR inhibitor treatment (Figure 1B, panel 2). Overall, H-STS cells were

identified to be completely insensitive to RAD treatment and exhibited higher feedback activation compared with KRJ-I cells; this finding was confirmed by a significant decrease of *Ki67* transcripts in the primary versus metastatic cell line. This individual tumor cell response is suggestive of site-specific (localized versus metastatic) differences in the pathobiological function of SI NETs and emphasizes the importance of an individualized treatment based on a biotherapeutic (signal transduction) response profile.

Treatment with OCT demonstrated no significant differences in any of the signaling pathway protein levels measured, suggesting that the antiproliferative effects of OCT, though relatively modest (<10%), are not based on perturbations in the PI3K–AKT–mTOR pathway. Interestingly, the combination approach demonstrated no significant difference in PI3K/AKT/mTOR signaling in either cell line, confirming that somatostatin receptor activation does not affect signaling through these pathways.

Activation of AKT as well as ERK1/2 by targeting mTORC1 is caused through up-regulation of growth factor and growth factor receptor synthesis and secretion.^{19,24} Serotonin is known to play an autocrine role in SINET proliferation^{33,41} and was significantly decreased by any of the 3 treatments in KRJ-I cells and only after OCT treatment in H-STS cells. Importantly, a significant increase in IGF-1 secretion and receptor transcription was evident in both cell lines; increased receptor protein levels as well as receptor activation were noted in the metastatic cell line. Because SINETs are known to respond to IGF-1 with increased proliferation,⁴² these data demonstrate that up-regulation of IGF-1 receptors and IGF-1 secretion results in growth factor–mediated tumor cell escape, particularly in liver metastasis. In preliminary analyses, we identified up-regulation of IGF-1 receptor as well as phosphorylation of IGF-IR and AKT (at Ser473) in a liver metastasis from a NET patient treated with OCT (unpublished data). This particular lesion had a *Ki67* >2%, suggesting that faster proliferating tumors may not be as amenable to biotherapeutics as slow-growing lesions. The antiproliferative effects of somatostatin analogs noted in the PROMID study was limited to slow-growing (*Ki67* <2%) tumors that were largely indolent.³⁹ In addition, it is unclear how an analog may function together with an mTOR inhibitor in this setting. Overall, liver metastases appear to have the machinery to escape biotherapeutic intervention. Primary tumors, in contrast, may function differently. Interestingly, no significant effect on IGF-1 receptor protein expression was noted in the primary cell

line (KRJ-I), although an increase in IGF-1 receptor transcript levels was evident. We interpret this finding as reflecting either a delayed feedback response in the primary tumor (partially sensitive to RAD) or involvement of the TGF β pathway in growth regulatory escape based on increased messenger RNA transcripts of TGF β 2 receptor and TGF β 1 secretion noted only in the primary tumor. Primary tumors respond to TGF β 1 with proliferation, an effect we have reported previously.³⁶

In conclusion, our findings demonstrate that both primary and liver metastasis–derived SINET cell lines escape from mTOR inhibitor treatment based on a dual feedback activation of AKT and ERK1/2 via an increase in RTK receptors and growth factor secretion. Different response rates to the agent were identified, however, indicating the importance of an individualized tumor response profile to biotherapeutic agents. Treatment with OCT had no impact on the PI3K–AKT–mTOR pathway in both cell lines and failed to overcome the feedback activation. Dual targeting mTOR and ERK1/2 might provide an alternative method to reverse the feedback cross-activation and re-establish the antiproliferative effect of mTOR inhibitors in SINETs.

CONFLICT OF INTEREST DISCLOSURES

This work was supported by National Institutes of Health Grants CA097050 (to I. M. M.) and DK080871 (to M. K.)

REFERENCES

1. Modlin IM, Oberg K, Chung DC, et al. Gastroenteropancreatic neuroendocrine tumours. *Lancet Oncol*. 2008;9:61-72.
2. Yao JC, Hassan M, Phan A, et al. One hundred years after “carcinoid”: epidemiology of and prognostic factors for neuroendocrine tumors in 35,825 cases in the United States. *J Clin Oncol*. 2008;26:3063-3072.
3. Modlin IM, Kidd M, Latich I, Zikusoka MN, Shapiro MD. Current status of gastrointestinal carcinoids. *Gastroenterology*. 2005;128:1717-1751.
4. Guertin DA, Sabatini DM. Defining the role of mTOR in cancer. *Cancer Cell*. 2007;12:9-22.
5. Sawyers CL. Will mTOR inhibitors make it as cancer drugs? *Cancer Cell*. 2003;4:343-348.
6. Yao JC, Lombard-Bohas C, Baudin E, et al. Daily oral everolimus activity in patients with metastatic pancreatic neuroendocrine tumors after failure of cytotoxic chemotherapy: a phase II trial. *J Clin Oncol*. 2010;28:69-76.
7. Yao JC, Phan AT, Chang DZ, et al. Efficacy of RAD001 (everolimus) and octreotide LAR in advanced low- to intermediate-grade neuroendocrine tumors: results of a phase II study. *J Clin Oncol*. 2008;26:4311-4318.
8. Kim DH, Sarbassov DD, Ali SM, et al. mTOR interacts with raptor to form a nutrient-sensitive complex that signals to the cell growth machinery. *Cell*. 2002;110:163-175.
9. Kim DH, Sarbassov DD, Ali SM, et al. GbetaL, a positive regulator of the rapamycin-sensitive pathway required for the nutrient-sensitive interaction between raptor and mTOR. *Mol Cell*. 2003;11:895-904.
10. Hara K, Maruki Y, Long X, et al. Raptor, a binding partner of target of rapamycin (TOR), mediates TOR action. *Cell*. 2002;110:177-189.
11. Loewith R, Jacinto E, Wullschlegel S, et al. Two TOR complexes, only one of which is rapamycin sensitive, have distinct roles in cell growth control. *Mol Cell*. 2002;10:457-468.
12. Garami A, Zwartkruis FJ, Nobukuni T, et al. Insulin activation of Rheb, a mediator of mTOR/S6K/4E-BP signaling, is inhibited by TSC1 and 2. *Mol Cell*. 2003;11:1457-1466.
13. Inoki K, Li Y, Xu T, Guan KL. Rheb GTPase is a direct target of TSC2 GAP activity and regulates mTOR signaling. *Genes Dev*. 2003;17:1829-1834.
14. Zhang Y, Gao X, Saucedo LJ, Ru B, Edgar BA, Pan D. Rheb is a direct target of the tuberous sclerosis tumour suppressor proteins. *Nat Cell Biol*. 2003;5:578-581.
15. Sarbassov DD, Ali SM, Kim DH, et al. Rictor, a novel binding partner of mTOR, defines a rapamycin-insensitive and raptor-independent pathway that regulates the cytoskeleton. *Curr Biol*. 2004;14:1296-1302.
16. Sarbassov DD, Guertin DA, Ali SM, Sabatini DM. Phosphorylation and regulation of Akt/PKB by the rictor-mTOR complex. *Science*. 2005;307:1098-1101.
17. Foster DA, Toschi A. Targeting mTOR with rapamycin: one dose does not fit all. *Cell Cycle*. 2009;8:1026-1029.
18. Harrington LS, Findlay GM, Gray A, et al. The TSC1–2 tumor suppressor controls insulin-PI3K signaling via regulation of IRS proteins. *J Cell Biol*. 2004;166:213-223.
19. O’Reilly KE, Rojo F, She QB, et al. mTOR inhibition induces upstream receptor tyrosine kinase signaling and activates Akt. *Cancer Res*. 2006;66:1500-1508.
20. Shah OJ, Wang Z, Hunter T. Inappropriate activation of the TSC/Rheb/mTOR/S6K cassette induces IRS1/2 depletion, insulin resistance, and cell survival deficiencies. *Curr Biol*. 2004;14:1650-1656.
21. Zhang H, Cicchetti G, Onda H, et al. Loss of Tsc1/Tsc2 activates mTOR and disrupts PI3K-Akt signaling through downregulation of PDGFR. *J Clin Invest*. 2003;112:1223-1233.
22. Wan X, Harkavy B, Shen N, Grohar P, Helman LJ. Rapamycin induces feedback activation of Akt signaling through an IGF-1R-dependent mechanism. *Oncogene*. 2007;26:1932-1940.
23. Carracedo A, Baselga J, Pandolfi PP. Deconstructing feedback-signaling networks to improve anticancer therapy with mTORC1 inhibitors. *Cell Cycle*. 2008;7:3805-3809.
24. Carracedo A, Ma L, Teruya-Feldstein J, et al. Inhibition of mTORC1 leads to MAPK pathway activation through a PI3K-dependent feedback loop in human cancer. *J Clin Invest*. 2008;118:3065-3074.
25. Shida T, Kishimoto T, Furuya M, et al. Expression of an activated mammalian target of rapamycin (mTOR) in gastroenteropancreatic neuroendocrine tumors. *Cancer Chemother Pharmacol*. 2010;65:889-893.
26. Zitzmann K, Ruden J, Brand S, et al. Compensatory activation of Akt in response to mTOR and Raf inhibitors—a rationale for dual-targeted therapy approaches in neuroendocrine tumor disease. *Cancer Lett*. 2010;295:100-109.

27. Modlin IM, Kidd M, Pfragner R, Eick GN, Champaneria MC. The functional characterization of normal and neoplastic human enterochromaffin cells. *J Clin Endocrinol Metab.* 2006;91:2340-2348.
28. Kidd M, Eick GN, Modlin IM, Pfragner R, Champaneria MC, Murren J. Further delineation of the continuous human neoplastic enterochromaffin cell line, KRJ-I, and the inhibitory effects of lanreotide and rapamycin. *J Mol Endocrinol.* 2007;38:181-192.
29. Kidd M, Drozdov I, Joseph R, Pfragner R, Culler M, Modlin I. Differential cytotoxicity of novel somatostatin and dopamine chimeric compounds on bronchopulmonary and small intestinal neuroendocrine tumor cell lines. *Cancer.* 2008;113:690-700.
30. Kidd M, Schally AV, Pfragner R, Malfertheiner MV, Modlin IM. Inhibition of proliferation of small intestinal and bronchopulmonary neuroendocrine cell lines by using peptide analogs targeting receptors. *Cancer.* 2008;112:1404-1414.
31. Pfragner R, Wirsnsberger G, Niederle B, et al. Establishment of a continuous cell line from a human carcinoid of the small intestine (KRJ-I): characterization and effects of 5-azacytidine on proliferation. *Int J Oncol.* 1996;8:513-520.
32. Pfragner R, Behmel A, Hoger H, et al. Establishment and characterization of three novel cell lines—P-STC, L-STC, H-STC - derived from a human metastatic midgut carcinoid. *Anticancer Res.* 2009;29:1951-1961.
33. Svejda B, Kidd M, Giovinazzo F, et al. The 5-HT(2B) receptor plays a key regulatory role in both neuroendocrine tumor cell proliferation and the modulation of the fibroblast component of the neoplastic microenvironment. *Cancer.* 2010;116:2902-2912.
34. Mosmann T. Rapid colorimetric assay for cellular growth and survival: application to proliferation and cytotoxicity assays. *J Immunol Methods.* 1983;65:55-63.
35. Ngamwongsatit P, Banada PP, Panbangred W, Bhunia AK. WST-1-based cell cytotoxicity assay as a substitute for MTT-based assay for rapid detection of toxigenic *Bacillus* species using CHO cell line. *J Microbiol Methods.* 2008;73:211-215.
36. Kidd M, Modlin IM, Pfragner R, et al. Small bowel carcinoid (enterochromaffin cell) neoplasia exhibits transforming growth factor-beta1-mediated regulatory abnormalities including up-regulation of C-Myc and MTA1. *Cancer.* 2007;109:2420-2431.
37. Kidd M, Eick G, Shapiro MD, Camp RL, Mane SM, Modlin IM. Microsatellite instability and gene mutations in transforming growth factor-beta type II receptor are absent in small bowel carcinoid tumors. *Cancer.* 2005;103:229-236.
38. Kidd M, Nadler B, Mane S, et al. GeneChip, geNorm, and gastrointestinal tumors: novel reference genes for real-time PCR. *Physiol Genomics.* 2007;30:363-370.
39. Rinke A, Muller HH, Schade-Brittinger C, et al. Placebo-controlled, double-blind, prospective, randomized study on the effect of octreotide LAR in the control of tumor growth in patients with metastatic neuroendocrine midgut tumors: a report from the PROMID Study Group. *J Clin Oncol.* 2009;27:4656-4663.
40. Sarbassov DD, Ali SM, Sengupta S, et al. Prolonged rapamycin treatment inhibits mTORC2 assembly and Akt/PKB. *Mol Cell.* 2006;22:159-168.
41. Drozdov I, Kidd M, Gustafsson BI, et al. Autoregulatory effects of serotonin on proliferation and signaling pathways in lung and small intestine neuroendocrine tumor cell lines. *Cancer.* 2009;115:4934-4945.
42. Nilsson O, Wangberg B, Theodorsson E, Skottner A, Ahlman H. Presence of IGF-I in human midgut carcinoid tumours—an autocrine regulator of carcinoid tumour growth? *Int J Cancer.* 1992;51:195-203.